JOURNAL OF GEOPHYSICAL RESEARCH, VOL. 101, NO. D4, PAGES 9079–9091, APRIL 20, 1996

Simulating equilibrium within aerosols and nonequilibrium between gases and aerosols

Mark Z. Jacobson

Department of Civil Engineering, Terman Engineering Center, Stanford University, Stanford, California

Azadeh Tabazadeh

NASA Ames Research Center, Mountain View, California

Richard P. Turco

Deptartment of Atmospheric Sciences, University of California, Los Angeles

Abstract. A numerical method to solve chemical equilibrium equations and a method of coupling the equilibrium calculations to nonequilibrium growth and evaporation are discussed. The equilibrium program solves any number of equations for gas, aqueous, ionic, and solid equilibrium concentrations over large spatial grids and particle size grids. It also simultaneously computes electrolyte mean mixed activity coefficients and aerosol liquid water content. Mean mixed activity coefficient calculations require mean binary activity coefficient information. Temperature-dependent mean binary activity coefficient polynomials were constructed using mean binary activity coefficient data at 298 K, apparent molal enthalpy data, and apparent molal heat capacity data. The equilibrium solver is mole and charge conserving, requires iteration, but always converges. Solutions to the equilibrium equations are used for two purposes. The first is to estimate surface vapor pressures over particles containing a solution and/or a solid phase. Such vapor pressures are then applied in gas-aerosol transfer equations. The second is to estimate intraparticle composition and size immediately after gas-aerosol transfer.

1. Introduction

Aerosols are important in many regions of the atmosphere. For example, near the surface, aerosols impede visibility, serve as hosts for acid-producing chemical reactions, and impair human health. In the stratosphere, aerosol constituents catalyze chemical reactions that can produce ozone-depleting gases. Numerically simulating the composition and size of atmospheric aerosols requires a model that treats many processes. Among these are emissions, nucleation, coagulation, growth, evaporation, chemical equilibrium, aqueous chemistry, deposition, transport, and radiation. Here, the coupling of chemical equilibrium to gas-aerosol transfer calculations is discussed.

Reversible chemical equilibrium equations are often used to determine the relationship among and between dissolved species molalities, dissociated ion molalities, solid mole concentrations, and particle surface vapor pressures. A "particle surface vapor pressure" is the pressure exerted by a gas just above the particle surface, whereas the "partial pressure" of the gas is the pressure exerted by the gas far removed from the particle surface. When only growth and one particle are considered, gas far removed from the particle diffuses toward and may deposit on, condense on, or dissolve in the particle until the partial pressure of the gas equals the particle surface vapor pressure. At that point, the system as a whole may be considered in equilibrium or steady state, and the partial pressure of the gas may be defined as the "partial pressure of the gas at equilibrium."

With respect to atmospheric aerosols, *Stelson et al.* [1979] proposed that the partial pressures of ammonia and nitric acid could be considered in equilibrium with solid ammonium nitrate within particles. Many other studies have since examined gas-solid as well as gas-aqueous, aqueous-ion, and aqueous-solid atmospheric equilibrium reactions [*e.g.*, *Scott and Cattell*, 1979; *Stelson and Seinfeld*, 1982a, b, c; *Seigneur*, 1982; *Seigneur et al.*, 1984; *Russell et al.*, 1983, 1988; *Saxena and Peterson*, 1981; *Saxena et al.*, 1983, 1986, 1993; *Bassett and Seinfeld*, 1983, 1984; *Hildemann et al.*, 1984; *Russell and Cass*, 1986; *Pilinis et al.*, 1987; *Pilinis and Seinfeld*, 1987, 1988; *Wexler and Seinfeld*, 1990, 1991, 1992; *Kim et al.*, 1993a, b].

Allen *et al.* [1989] suggested that under some conditions the assumption of equilibrium between solid ammonium nitrate and ammonium chloride aerosols and the gas phase may not always be valid. Subsequently, *Harrison and MacKenzie* [1990] and *Wexler and Seinfeld* [1990] supported this hypothesis. Furthermore, *Wexler and Seinfeld* [1991] discussed equations for simulating both transport of gas to and equilibrium treatment within electrolyte-containing aerosols.

Here, growth equations are also used to transport gases to particle surfaces, and such equations are given. Further, a new equilibrium solver (EQUISOLV) and polynomial expressions for temperature-dependent activity coefficients are described. Recently, *Tabazadeh et al.* [1994a] derived binary activity coefficient data for cold stratospheric temperatures. They applied EQUISOLV along with the low-temperature activity coefficients to study stratospheric aerosol composition. Similarly, *Tabazadeh*

Paper number 96JD00348.
0148-0227/96/96JD-00348$05.00

et al. [1994b] and *Drdla et al.* [1994] used the model with the cold-temperature activity coefficients to study the formation of polar stratospheric clouds.

2. Surface Vapor Pressure Estimates

A key component in the gas-aerosol transfer equation is the particle surface vapor pressure. In the case of sulfuric acid, where the surface vapor pressure is very low and the Henry's constant is not well known, the vapor pressure can be estimated empirically [*e.g., Bolsaitis and Elliott,* 1990]. Also, in the case of water vapor the surface vapor pressure is a strong function of temperature and can be estimated empirically when the relative humidity exceeds 100% [*e.g., Bolton,* 1980]. On the other hand, when the relative humidity is less than 100%, aerosol liquid water content is primarily a function of dissociated ion molality. One way to estimate liquid water content in such cases is to assume that water vapor is in equilibrium with its liquid phase and to solve an empirical water equation.

For most species, however, the surface vapor pressure over a solution or solid can be estimated with reversible equilibrium relationships. For example, if a species does not exist in the solid phase but is dissolved in solution, the surface vapor pressure of the species equals its activity divided by its Henry's constant [*e.g., Schwartz and Freiberg,* 1981; *Schwartz,* 1984; *Chameides,* 1984; *Jacob,* 1986; *Pandis and Seinfeld,* 1989; *Bott and Carmichael,* 1993; *Wexler and Seinfeld,* 1991]. For example, if nitric acid transfers reversibly between the gas-aqueous interface via the reaction $HNO_3(g) \Leftrightarrow HNO_3(aq)$, then the particle surface vapor pressure (atm) of nitric acid is

$$p_{s,HNO_3(g)} = m_{HNO_3(aq)} \gamma_{HNO_3(aq)} / H_{HNO_3} \quad (1)$$

where $m_{HNO_3(aq)}$ is the molality (mol kg^{-1}), $\gamma_{HNO_3(aq)}$ is the activity coefficient (unitless), and H_{HNO_3} is the Henry's constant (mol kg^{-1} atm^{-1}) of dissolved, undissociated nitric acid. In this equation, $m_{HNO_3(aq)} \gamma_{HNO_3(aq)} = \{HNO_3(aq)\}$, which is the thermodynamic activity of nitric acid in solution. In this example the activity coefficient of nitric acid is assumed to be unity. As more nitric acid dissolves in the particle, it dissociates and water content increases due to hydration. However, the net molality of undissociated nitric acid increases, increasing the particle surface vapor pressure via equation (1).

If a species is in the solid phase on part of the surface of a particle and is dissolved in water on the rest of the surface and if the solid phase is in equilibrium with the solution phase, the surface vapor pressure of the species over the solid is calculated to be the same as that over the solution and can be estimated from a Henry's law equation. For example, suppose a system consists of $HNO_3(g)$, $NH_3(g)$, $HNO_3(aq)$, $NH_3(aq)$, and $NH_4NO_3(s)$ (ignoring dissociated ions for the time being). In this case, the surface vapor pressure product over the solid is constrained by

$$p_{s,NH_3(g)} p_{s,HNO_3(g)} = K_{eq,NH_4NO_3(s)} \quad (2)$$

where $p_{s,NH_3(g)}$ is the particle surface vapor pressures of ammonia and $K_{eq,NH_4NO_3(s)}$ is the equilibrium coefficient of solid ammonium nitrate with respect to the gas phase. Further, the surface vapor pressure of $HNO_3(g)$ over the solution is controlled by equation (1) while that of $NH_3(g)$ is controlled by the Henry's law relation,

$$p_{s,NH_3(g)} = m_{NH_3(aq)} \gamma_{NH_3(aq)} / H_{NH_3} . \quad (3)$$

where $\gamma_{NH_3(aq)}$ is the activity coefficient of undissociated, dissolved ammonia, also assumed to be unity in this example. In addition, equations (1) and (3) can be substituted into equation (2) to give the solution-solid equilibrium coefficient equation,

$$m_{NH_3(aq)} m_{HNO_3(aq)} = H_{NH_3} H_{HNO_3} K_{eq,NH_4NO_3(s)} \quad (4)$$

where activity coefficients were removed for simplicity. Finally, mass balance within the particle requires

$$m_{NH_3(aq)} w_{H_2O(aq)} + c_{NH_4NO_3(s)} = c_{tot,NH_3} \quad (5)$$

$$m_{HNO_3(aq)} w_{H_2O(aq)} + c_{NH_4NO_3(s)} = c_{tot,HNO_3} \quad (6)$$

where $w_{H_2O(aq)}$ is liquid water content (kg water cm^{-3} air), assumed constant and known for now, $c_{NH_4NO_3(s)}$ is the ammonium nitrate mole concentration (mol cm^{-3} air), and the c_{tot} values are the initial mole concentrations of the solid plus dissolved phases of the species, which are given as initial conditions.

At any given time, the solution to equations (4) - (6) gives the internal equilibrium distribution of $m_{NH_3(aq)}$, $m_{HNO_3(aq)}$, and $c_{NH_4NO_3(s)}$. Further, equations (1) and (3) give the surface vapor pressures of nitric acid and ammonia gas, respectively. Such vapor pressures automatically satisfy equation (2) since equation (4) was derived from equations (1) - (3). Consequently, ammonia and nitric acid's surface vapor pressures over the solid phase are calculated to be equal to their respective vapor pressures over the solution phase when the solution and solid are assumed to be in equilibrium with each other.

Suppose, for example, that an equilibrium atmosphere (where surface vapor pressures over the solid and dissolved phases in a single particle are identical) is perturbed with additional ammonia gas. The gas diffuses to and dissolve into the particle, increasing c_{tot,NH_3}. Immediately, a new internal equilibrium is established and determined by solving equations (4) - (6). The result is an increase in $m_{NH_3(aq)}$ and $c_{NH_4NO_3(s)}$ and a decrease in $m_{HNO_3(aq)}$. Consequently, $p_{s,NH_3(g)}$ increases via equation (3) and $p_{s,HNO_3(g)}$ decreases via equation (1); however, the product $p_{s,NH_3(g)} p_{s,HNO_3(g)}$ remains constant since equation (4) is satisfied. Thus, the calculated surface vapor pressures over the solution satisfy the surface vapor pressure constraint over the solid phase.

In nearly all cases in which electrolytes are present, even at relative humidities less than 10%, particles contain at least a minute amount of water, (*e.g.*, even 10^{-7} $\mu g\ m^{-3}$ or less) is present. For the most part, the only time that an electrolyte-containing particle is completely dry is when no dissociated ions exist in solution. In such cases, all electrolyte mass is usually in the form of solid(s). When even a small amount of liquid water is present on the surface of a particle and the solution phase is assumed to be in equilibrium with the solid phase, particle surface vapor pressures can be estimated by solving internal equilibrium and applying a Henry's constant to the aqueous molalities, as described above.

However, when only solids (and zero liquid water) exist, the surface vapor pressures can also be estimated by assuming a negligible amount of water on the particle surface and solving the same equations that arise when solids coexist with the solution phase. In such cases, the choice of the level of liquid water content is immaterial since the surface vapor pressures will be the same, regardless of the amount. For example, in the above problem, suppose that only $NH_4NO_3(s)$ exists in the particle. Consequently, $c_{tot,HNO_3} = c_{tot,NH_3}$. Now, assume that a

negligible amount of liquid water is present on the particle surface. Regardless of the amount, equations (5) and (6) simplify to $m_{HNO_3(aq)} = m_{NH_3(aq)}$. Applying this result to equation (4) gives

$$m_{HNO_3(aq)} = m_{NH_3(aq)} = \sqrt{H_{NH_3} H_{HNO_3} K_{eq,NH_4NO_3(s)}} \cdot \quad (7)$$

Consequently, the particle surface vapor pressures can be estimated from equations (1) and (3). This methodology can be applied to multiple solids existing simultaneously. However, there is no need to solve each case separately. Instead, an equilibrium solver, such as the one described below, can be used to solve all internal aerosol equilibrium equations simultaneously. During this calculation, the water content, solid concentrations, and molalities are determined. In almost all cases some liquid water exists, even if it is a minute amount. So long as a minimum liquid water content is specified in the cases when water disappears, equilibrium molalities are calculated. Such molalities are then used to estimate particle surface vapor pressures via Henry's constant equations.

In sum, the surface vapor pressure of a species over both its solid and solution surfaces can often be estimated numerically by first assuming that the solid and solution phases are in equilibrium with each other and then solving internal particle equilibrium equations together. A surface vapor pressure is determined by applying a Henry's constant to an internal equilibrium molality, even when solids coexist with the solution phase. If the water equation predicts zero liquid water but solid electrolytes are present, the surface vapor pressures over these electrolytes can be estimated by assuming that a minute amount of water exists on the surface, adjacent to the solids, and solving the same equilibrium equations as in the other cases.

3. Gas-Particle Transfer Equations

The equation for mass transfer between the gas and the particle phases combined with the change in particle composition due to reversible reactions can be written as

$$\frac{dc_{i,q,t}}{dt} = k_{i,q}\left(C_{q,t} - B_{i,q} C_{s,i,q,t}\right) - \left(\frac{dc_{i,q,t}}{dt}\right)_{eq}, \quad (8)$$

where $c_{i,q,t}$ is the mole concentration of species q in size bin i at time t (mol cm^{-3} air), $C_{q,t}$ is the partial vapor concentration of species q in the gas phase (mol cm^{-3} air), $C_{s,i,q,t}$ is the particle surface vapor concentration (mol cm^{-3} air), $k_{i,q}$ is the mass transfer rate between the gas phase and all particles of size i (s^{-1}), $B_{i,q}$ is a Kelvin effect term (unitless), and $\left(dc_{i,q,t}/dt\right)_{eq}$ is the rapid change in particle concentration of the species due to reversible equilibrium reactions within the particle (*e.g.*, dissociation, precipitation).

The mass transfer rate can be estimated as $k_{i,q} = n_i 4\pi r_i D_{q,i}^{eff}$, where n_i is the number concentration of particles of size i (particles cm^{-3}), r_i is the radius of a single particle, and $D_{q,i}^{eff}$ is an effective diffusion coefficient (cm^2 s^{-1}) that accounts for the geometry of vapor collision with small particles and ventilation of heat and vapor during sedimentation of large particles containing liquid water [*e.g.*, *Jacobson and Turco*, 1995].

The corresponding equation for mass conservation between the gas and all size bins of the particle phase is

$$\frac{dC_{q,t}}{dt} = -\sum_{i=1}^{N_B}\left[k_{i,q}\left(C_{q,t} - B_{i,q} C_{s,i,q,t}\right) - \left(\frac{dc_{i,q,t}}{dt}\right)_{eq}\right], \quad (9)$$

where N_B is the number of particle size bins.

At any given instant, the surface vapor pressure of a soluble species can be set equal to the molality of the species divided by its Henry's constant, so long as at least a small amount of liquid water is in equilibrium with the solid phase. Thus, in such cases,

$$C_{s,i,q,t} = \frac{c_{i,q,t}}{H'_q} = \frac{m_{i,q,t}\gamma_i}{1000 R_u T H_q}, \quad (10)$$

where R_u is the universal gas constant (L atm^{-1} mole^{-1} K^{-1}), T is temperature (K), $H'_q = M_q c_{i,w,t} R_u T H_q$, γ_i is the activity coefficient of the undissociated, dissolved species, and

$$c_{i,q,t} = M_w m_{i,q,t} \gamma_i c_{i,w,t} / 1000. \quad (11)$$

In these equations, $c_{i,w,t}$ is the liquid water mole concentration (mol cm^{-3}), M_q is the molecular weight of species q, and M_w is the molecular weight of water. Equation (10) can be inserted into equations (8) and (9) to yield

$$\frac{dc_{i,q,t}}{dt} = k_{i,q}\left(C_{q,t} - B_{i,q}\frac{c_{i,q,t}}{H'_q}\right) - \left(\frac{dc_{i,q,t}}{dt}\right)_{eq} \quad (12)$$

$$\frac{dC_{q,t}}{dt} = -\sum_{i=1}^{N_B}\left[k_{i,q}\left(C_{q,t} - B_{i,q}\frac{c_{i,q,t}}{H'_q}\right) - \left(\frac{dc_{i,q,t}}{dt}\right)_{eq}\right], \quad (13)$$

respectively.

If solids coexist with the solution phase, then the dissolution of additional material into the particle may or may not affect species molality. For example, if ammonium nitrate solid is in equilibrium with the solution phase and additional ammonia gas dissolves, then the molality of dissolved ammonia (and ammonium ion) increases, the concentration of solid ammonium nitrate increases, and the molality of dissolved nitric acid (and nitrate ion) decreases. However, if both nitric acid and ammonia gases dissolve in the correct proportions, additional solid precipitates and the molalities of dissolved nitric acid and ammonia gases do not change. The exchange of mass during either case is accounted for in the $\left(dc_{i,q,t}/dt\right)_{eq}$ term. Thus, the current value of $c_{i,q,t}/H'_q$ in equations (11) and (12) depends significantly on $\left(dc_{i,q,t}/dt\right)_{eq}$.

In most atmospheric modeling cases the $\left(dc_{i,q,t}/dt\right)_{eq}$ term must be solved separately from the growth term and relatively infrequently. Ideally, when the growth term is solved by integratation, equilibrium is solved after each time step of the growth integration. For example, suppose a 15-min. time period requires 50 integration time steps for growth. After each growth step, the equilibrium equations should be solved. However, while such calculations can be performed on a small scale, they are currently difficult to perform in a large Eulerian model. Consequently, the equilibrium step is usually solved during intermittent growth integration time steps. The code used here to integrate the growth equations is a sparse-matrix ordinary differential equation solver [*Jacobson*, 1995]. Such a code is useful for solving growth equations because the matrix of growth equation partial derivatives is sparse.

A remaining issue is whether $c_{i,q,t}/H'_q$ should be allowed to vary during the integration of growth or whether it should be set to $c_{i,q,t-1}/H'_q$, where the subscript t-1 indicates the value at the end of the last equilibrium update. If the term varies in equations (12) and (13), then the surface vapor pressure increases as more gas dissolves in the particle, slowing down the rate of transfer to the particle. This situation is realistic when particles contain only liquid water. If the term remains constant, then the difference

between partial and surface vapor pressures remains constant during the time interval, which is realistic if gases dissolve in such proportions so as to completely precipitate upon dissolution.

Here, it is assumed that when a species does not precipitate in solution or react on a surface to form a solid, the term $c_{i,q,t}/H'_q$ is allowed to vary during the integration of growth. Also, when a species can form a solid, but the ambient relative humidity is greater than the highest deliquescence relative humidity of all possible solids that the species may form, $c_{i,q,t}/H'_q$ is allowed to vary. However, when the relative humidity is below this maximum deliquescence relative humidity, the term $c_{i,q,t-1}/H'_q$ is used in equations (12) and (13).

4. Chemical Equilibrium Solution

To estimate either surface vapor pressures or internal particle composition and size, a chemical equilibrium solver (EQUISOLV) was developed. The code solves any number of aqueous-ion, aqueous-solid, ion-ion, ion-solid, solid-solid, gas-solid, gas-aqueous, and gas-ion equilibrium equations simultaneously. However, for surface vapor pressure or internal composition calculations, all gas-related reactions are neglected. The code also calculates mixed mean activity coefficients and aerosol water content.

At least two types of methods have previously been used to solve equilibrium, activity coefficient, and water equations together. These include bisectional-Newton methods [*Pilinis and Seinfeld*, 1987; *Kim et al.*, 1993a, b] and methods that minimize free energy [*Bassett and Seinfeld*, 1983, 1984; *Wexler and Seinfeld*, 1990]. EQUISOLV and these other methods require iteration and are mass and charge conserving.

Characteristics of EQUISOLV are its simplicity and its relative speed in three-dimensional simulations. Also, the code can converge thousands of equilibrium equations simultaneously without fear of negative concentrations. This characteristic permits continuous solutions over large numbers of spatial size grids and particles size bins.

In addition, the method requires no intelligent first guess. The only constraints are that the system must start in charge balance and the sum of moles of each atom must equal the total number of desired moles of a component in the system. For example, if the total nitrate in the system is known to be 20 $\mu g\ m^{-3}$, then the nitrate can be distributed initially, in any proportion, among $HNO_3(aq)$, NO_3^-, $NH_4NO_3(s)$, etc. Similarly, the charge balance constraint allows initial charges to be distributed among all dissociated ions, except that the sum, over all species, of charge multiplied by molality must equal zero. The simplest way to initialize charge is to set all ion molalities to zero. However, components can be initialized subject to the constraints in numerous ways that can be automatized in the computer program.

Further, EQUISOLV is mass and charge conserving at all times, regardless of when the iterations stop. The only requirement is that the equilibrium equations must be written in a mass- and charge-conserving manner. For example, the equation $HNO_3(aq) \Leftrightarrow H^+ + NO_3^-$ conserves mass and charge. Finally, while the code solves any number of equilibrium equations together, new equations are not wired into the code. To the contrary, all equilibrium equations are written into an input file, and the code automatically organizes the equations into appropriate arrays that are fed into the solution portion of the code.

The code consists of a scheme that uses part of a method from Villars [1959]. This method requires the solution one equilibrium equation at a time by iteration. To solve a system of equations, all equations are iterated many times. For example, suppose a system consists of a single aerosol size bin and 15 equations representing the equilibrium chemistry within that bin (the gas phase is neglected here). At the start, the first equation is iterated. When the first equation converges, the updated and other initial concentrations are used as inputs into the second equation. This continues until the fifteenth equation has converged. At that point, concentrations from the first equation are no longer in equilibrium. Thus, the sequence is repeated, from the first to fifteenth equation, over and over, until concentrations no longer change upon more iteration.

Equilibrium among multiple particle size bins and the gas phase can also be solved in a similar manner. For example, suppose a system consists of 50 size bins, 15 equations per bin, and 3 gas species that equilibrate with aqueous phase species in each bin. Beginning with the first bin, each equation is iterated until convergence occurs for that equation. If the equilibrium equation includes a gas, the gas concentration is updated until the equation converges. After the equations in the first bin are iterated and converged, the equations in the second bin are iterated. The updated gas concentrations from the first bin affect the equilibrium distribution in the second size bin and, conversely, the equilibrium distribution in the second bin affects the gas phase. After the last size bin is iterated, the sequence of iterations is repeated in reverse order, from the fiftieth to the first bin. The marches back and forth among the size bins continue until gas and aerosol concentrations do not change from iteration to iteration. While equilibrium solutions between the gas and the aerosol phases can be found, they are unnecessary if the gas phase is assumed not to be in equilibrium with the aerosol phase. In such cases, growth equations are used to transfer the species between the two phases. Further, in some special cases the equilibrium solution between the gas phase and the particle phases may not be unique.

4.1. Basic Mechanism

Here, the iteration sequence for one equilibrium equation is discussed. For this description all subscripts identifying particle type and size bin are omitted. The general structure of an equilibrium equation is

$$\nu_D D + \nu_E E + \cdots \Leftrightarrow \nu_A A + \nu_B B + \cdots, \tag{14}$$

where the ν values are the number of moles of each gas, aqueous, ion, or solid reactant or product and D, E, A, and B are the chemical symbols of the reactants and products.

The relationship among the equilibrium constant ($K_{eq}(T)$), the stoichiometric coefficients, and the reactant and product activities in equation (14) is

$$\frac{\{A\}^{\nu_A}\{B\}^{\nu_B}\ldots}{\{D\}^{\nu_D}\{E\}^{\nu_E}\ldots} = K_{eq}(T), \tag{15}$$

where $\{A\}$, ..., are the thermodynamic activities of A, ... These activities measure the effective concentration or intensity of the substance. The activity of a gas is its partial pressure; the activity of an ion in solution is its molality multiplied by its activity coefficient (γ) (unitless); the activity of an undissociated electrolyte is its molality; the activity of liquid water in the atmosphere is the ambient relative humidity (fraction); and the activity of a solid is unity.

In the code all concentrations for gas, aqueous, ionic, and solid species are set in units of moles concentration (mol cm^3 air). The

conversion of aqueous or ionic mole concentration units to molality units was given in equation (11). Similarly, the conversion of gas mole concentration units to pressure units is $p_q = 1000 C_q R_u T$, where p_q is the partial pressure (atm) of gas q. If surface vapor pressures are solved for, then only internal equilibrium equations are determined, and a Henry's constant is applied to aqueous molalities. Thus, in such cases, partial pressures are not used.

To demonstrate the solution to one equilibrium equation, an example where two gases equilibrate with two ions is shown. The sample equation has the form of equation (14), with two gases on the left side of the equation. The first step is to calculate Q_d and Q_n the smallest ratio of mole concentration to moles among species appearing in the denominator and numerator, respectively, of equation (15). Thus,

$$Q_d = \mathrm{MIN}\left\{\frac{C_{D,1}}{\nu_D}, \frac{C_{E,1}}{\nu_E}\right\} \tag{16}$$

$$Q_n = \mathrm{MIN}\left\{\frac{c_{A,1}}{\nu_A}, \frac{c_{B,1}}{\nu_B}\right\}, \tag{17}$$

where the superscript "1" refers to initial concentration. Initial concentrations can be selected randomly with the requirement that moles of all individual species in a mole-balance group must sum up to the total moles in the group. If an equilibrium equation contains a solid, each solid's concentration is included in equation (16) or equation (17). By putting species of all physical states in the same units, confusion is avoided in these and subsequent calculations.

Next, two parameters are initialized as $z_1 = 0.5(Q_d + Q_n)$ and $\Delta x_1 = Q_d - z_1$. The iteration begins by adding the mass flux factor (Δx, which may be positive or negative) to each mole concentration in the numerator or subtracting it from each mole concentration in the denominator of the equilibrium equation. Thus,

$$c_{A,l+1} = c_{A,l} + \nu_A \Delta x_l \qquad c_{B,l+1} = c_{B,l} + \nu_B \Delta x_l \tag{18}$$

$$C_{D,l+1} = C_{D,l} - \nu_D \Delta x_l \qquad C_{E,l+1} = C_{E,l} - \nu_E \Delta x_l. \tag{19}$$

respectively. Starting with equation (18), iteration numbers are referred to by superscripts l and l+1. If the equation contain solids, then the change of each solid's concentration is calculated the same way as in equation (18) or equation (19) (solid, aqueous, and ionic mole concentrations are all identified with a c). The above equations show that during each iteration, mass and charge are transferred either from reactants to products or vice-versa. This transfer continues until $\Delta x = 0$. Thus, the scheme conserves mass and charge each iteration.

Next, the updated ratio of activities is compared to the equilibrium constant. The ratio is

$$F = \left[\frac{\left(m_{A,l+1}\right)^{\nu_A}\left(m_{B,l+1}\right)^{\nu_B}\left(\gamma_{AB,l+1}\right)^{\nu_A+\nu_B}}{\left(p_{D,l+1}\right)^{\nu_D}\left(p_{E,l+1}\right)^{\nu_E}}\right] \Big/ K_{eq}(T). \tag{20}$$

To perform this calculation, mole concentrations are converted to either molality or atmospheres. In the case of solids the activities are unity; thus, none will appear in equation (20). Further, mixed mean activity coefficients (*e.g.*, $\gamma_{AB,l+1}$) are updated before each iteration sequence. They converge after all iteration sequences are complete. Finally, the liquid water content (c_w) is updated either during or before each iteration sequence.

In the final steps of the iteration, the value $z_{l+1} = 0.5 z_l$ is calculated and convergence is checked. The convergence criterion is

$$F = \begin{cases} >1 & \rightarrow \quad \Delta x_{l+1} = -z_{l+1} \\ <1 & \rightarrow \quad \Delta x_{l+1} = +z_{l+1} \\ =1 & \rightarrow \quad \text{convergence} \end{cases}. \tag{21}$$

Each nonconvergence Δx is updated, the iteration number is advanced, and the code returns to equation (18). Ultimately, all molalities converge to a positive number.

4.2. Temperature-Dependent Ion Activity Coefficients

Activity coefficients correct for the deviation from ideal behavior of a solution. To calculate mean activity coefficients for electrolytes in a multicomponent solution, Bromley's [1973] model, as described by *Pilinis and Seinfeld* [1987] is used. This method requires mean binary activity coefficient data.

Mean binary activity coefficient data at 298 K were obtained from a variety of sources, listed in Table 1. Among the sources were measurements from *Hamer and Wu* [1972] and parameters from *Pitzer* [1991]. Figure 1 compares mean binary coefficients obtained from these two sources for three species. The measured data are often accurate to high molality, while the Pitzer parameters are valid up to about 6 m. Since the aerosols of interest are usually concentrated, measured values were frequently used here. In most cases the mean binary activity coefficients were fit to polynomials of the form

$$\ln \gamma^0_{12b} = B_0 + B_1 m_{12}^{1/2} + B_2 m_{12} + B_3 m_{12}^{3/2} + \cdots, \tag{22}$$

where γ^0_{12b} is the mean binary activity coefficient of electrolyte "12" at 298 K, m is the molality of the electrolyte alone in solution at the same ionic strength as the mixture, and B_0, B_1, ... are fitting coefficients for the polynomial.

The temperature dependence of the electrolyte activity coefficients [*e.g.*, *Harned and Owen*, 1958; *Stelson et al.*, 1984; *Bassett and Seinfeld*, 1983; *Clegg and Brimblecombe*, 1990; *Tabazadeh et al.*, 1994] can be rewritten as

$$\ln \gamma_{12b}(T) = \ln \gamma^0_{12b} + \frac{T_L}{(\nu_1+\nu_2)R^* T_0}\left[\phi_L + m\frac{\partial \phi_L}{\partial m}\right] + \frac{T_C}{(\nu_1+\nu_2)R^*}\left[\phi_{c_p} + m\frac{\partial \phi_{c_p}}{\partial m} - \phi^o_{c_p}\right], \tag{23}$$

where $\gamma_{12b}(T)$ is the binary activity coefficient of the electrolyte at temperature T, T_0 is the reference temperature (298 K), R *is the gas constant (J mol^{-1} K^{-1}), ϕ_L is the relative apparent molal enthalpy (J mole^{-1}) of the species at molality m (where the subscript 12 has been omitted), ϕ_{c_p} is the apparent molal heat capacity (J mole^{-1} K^{-1}) at molality m, and $\phi^o_{c_p}$ is the apparent molal heat capacity at infinite dilution. Furthermore, $T_L = (T_0/T) - 1$ and $T_C = 1 + \ln(T_0/T) - (T_0/T)$ are temperature-dependent parameters.

The relative apparent molal enthalpy equals the negative of the heat of dilution, ΔH_D. Table 1 lists several sources of data for heat of dilution and apparent molal heat capacity. With these data, polynomials were constructed of the form

$$\phi_L = U_1 m^{1/2} + U_2 m + U_3 m^{3/2} + \cdots \tag{24}$$

$$\phi_{c_p} = \phi^o_{c_p} + V_1 m^{1/2} + V_2 m + V_3 m^{3/2} + \cdots. \tag{25}$$

Table 1. Parameters for Calculating Electrolyte Mean Binary Activity Coefficients

	index number	*Hamer and Wu* [1972]	*Parker* [1965]	*Parker* [1965]
		16 m	55.5 m	15.9 m
HCl	j	B_j	G_j	H_j
	0	-1.998104 (-2)	0	0
	1	-7.959068 (-1)	5.532198 (-1)	2.108728 (0)
	2	6.580198 (-1)	-2.571126 (-1)	8.542292 (-1)
	3	-7.409941 (-2)	2.790048 (-1)	-6.237459 (-1)
	4	1.345075 (-2)	-4.691631 (-2)	1.935911 (-1)
	5	-2.248651 (-3)	2.382485 (-3)	-2.037543 (-2)
		Hamer and Wu [1972]	*Parker* [1965]	*Parker* [1965]
		28 m	55.5 m	55.5 m
HNO_3	j	B_j	G_j	H_j
	0	-2.388378 (-2)	0	0
	1	-7.777787 (-1)	5.785894 (-1)	-4.785171 (-1)
	2	5.950086 (-1)	-9.860271 (-1)	6.521896 (0)
	3	-1.284278 (-1)	6.043012 (-1)	-2.605544 (0)
	4	1.291734 (-2)	-1.123169 (-1)	3.739984 (-1)
	5	-6.257155 (-4)	6.688134 (-3)	-1.832646 (-2)
		Hamer and Wu [1972]	*Parker* [1965]	*Perron et al.* [1981]
		6.1 m	6.1 m	6.0 m
NaCl	j	B_j	G_j	H_j
	0	-6.089937 (-3)	0	0
	1	-1.015184 (0)	5.808744 (-1)	2.261834 (0)
	2	9.345503 (-1)	-1.163239 (0)	3.622494 (0)
	3	-4.615793 (-1)	5.136893 (-1)	-1.608598 (0)
	4	1.431557 (-1)	-1.029523 (-1)	2.092972 (-1)
	5	-1.700298 (-2)	1.401488 (-2)	0
		Wu and Hamer [1980]	*Parker* [1965]	*Parker* [1965]
		10.8 m	9.2 m	2.2 m
$NaNO_3$	j	B_j	G_j	H_j
	0	-6.638145 (-3)	0	0
	1	-1.024329 (0)	5.678220 (-1)	7.232987 (-1)
	2	6.877457 (-1)	-2.136826 (0)	1.918907 (1)
	3	-3.336161 (-1)	1.145031 (0)	-2.382164 (1)
	4	8.387414 (-2)	-2.585350 (-1)	1.367081 (1)
	5	-8.154844 (-3)	2.390815 (-2)	-3.064556 (0)
		Harvie et al. [1984]	Used same as for NaCl	Used same as for NaCl
		6.0 m	6.1 m	6.0 m
$NaHSO_4$	j	B_j	G_j	H_j
	0	-8.890979 (-3)	0	0
	1	-9.559487 (-1)	5.808744 (-1)	2.261834 (0)
	2	8.758970 (-1)	-1.163239 (0)	3.622494 (0)
	3	-4.607380 (-1)	5.136893 (-1)	-1.608598 (0)
	4	1.309144 (-1)	-1.029523 (-1)	2.092972 (-1)
	5	-1.398546 (-2)	1.401488 (-2)	0
		Goldberg [1981]	*Wagman et al.* [1982]	*Holmes & Mesmer* [1986]
		4.4 m	3.1 m	2.0 m
Na_2SO_4	j	B_j	G_j	H_j
	0	-2.323071 (-2)	0	0
	1	-3.321509 (0)	1.698182 (0)	9.410224 (0)
	2	3.388793 (0)	-5.160108 (0)	2.213823 (1)
	3	-2.402946 (0)	2.132810 (0)	-3.481895 (1)
	4	8.926764 (-1)	8.840108 (-1)	2.348397 (1)
	5	-1.225933 (-1)	-5.143058 (-1)	-6.471345 (0)
		Hamer and Wu [1972]	*Wagman et al.* [1982]	*Parker* [1965]
		7.4 m	7.0 m	7.4 m
NH_4Cl	j	B_j	G_j	H_j
	0	-5.022484 (-3)	0	0
	1	-1.037873 (0)	4.890513 (-1)	1.959107 (0)
	2	8.517483 (-1)	-7.013315 (-1)	9.894682 (-1)
	3	-4.225323 (-1)	4.682151 (-1)	-1.024499 (-1)
	4	1.214996 (-1)	-1.702461 (-1)	-2.354376 (-1)
	5	-1.471525 (-2)	2.502643 (-2)	6.600384 (-2)

Table 1. (continued)

NH_4NO_3	j	*Hamer and Wu* [1972] 25.9 m B_j	*Vanderzee et al.* [1980] 25.0 m G_j	*Roux et al.* [1978] 22.4 m H_j
	0	-1.044572 (-2)	0	0
	1	-1.004940 (0)	4.362921 (-1)	2.611682 (0)
	2	4.674064 (-1)	-1.455444 (0)	3.158677 (0)
	3	-1.750495 (-1)	6.282104 (-1)	-2.005748 (0)
	4	3.253844 (-2)	-1.123507 (-1)	4.113737 (-1)
	5	-2.276789 (-3)	7.438990 (-3)	-2.820677 (-2)
NH_4HSO_4	j	*Bassett & Seinfeld* [1983] 6.0 m B_j	Used same as for NH_4Cl 7.0 m G_j	Used same as for NH_4Cl 7.4 m H_j
	0	-2.708121 (-3)	0	0
	1	-1.095646 (0)	4.890513 (-1)	1.959107 (0)
	2	1.042878 (0)	-7.013315 (-1)	9.894682 (-1)
	3	-6.289405 (-1)	4.682151 (-1)	-1.024499 (-1)
	4	2.079631 (-1)	-1.702461 (-1)	-2.354376 (-1)
	5	-2.776957 (-2)	2.502643 (-2)	6.600384 (-2)
$[NH_4]_2SO_4$	j	*Filippov et al.* [1985] 5.8 m B_j	*Wagman et al.* [1982] 5.5 m G_j	*Sukhatme and Saikhedkar* [1969] 5.5 m H_j
	0	-2.163694 (-2)	2.297972 (-1)	0
	1	-3.377941 (0)	4.255129 (-1)	1.609902 (-3)
	2	3.118007 (0)	-2.220594 (0)	4.437758 (0)
	3	-1.920544 (0)	2.607601 (0)	6.101756 (-3)
	4	6.372975 (-1)	-1.243384 (0)	4.021805 (-1)
	5	-8.277292 (-2)	2.102563 (-1)	4.375833 (-4)

Read 1.23 (0) as 1.23 x 10^0. The parameters fit into equation (27), which is subsequently used in equation (26). The B parameters (which also fit into equation (22)) give the activity coefficient at 298 K, the G parameters (described in the text) give the heat of dilution term, and the H parameters give the heat capacity term. The references identify the source of the data, and the molalities are the maximum values for either the activity coefficient data at 298 K, the heat of dilution data, or the heat capacity data.

Equation (24) does not include a U_0 term since $\phi_L = \phi_H - \phi_H^\circ$ (apparent molal enthalpy minus molal enthalpy at infinite dilution: infinite dilution occurs when $m = 0$).

Equations (23), (24), and (25) can be combined to give temperature-dependent, mean binary activity coefficient polynomials of the form

$$\ln\gamma_{12b}(T) = F_0 + F_1 m^{1/2} + F_2 m + F_3 m^{3/2} + \cdots, \quad (26)$$

where $F_0 = B_0$ and

$$F_j = B_j + G_j T_L + H_j T_C \quad (27)$$

for each additional term, beginning with j = 1. Also, $G_j = 0.5(j+2)U_j/\left[(\nu_1+\nu_2)R^*T_0\right]$ and $H_j = 0.5(j+2)V_j/\left[(\nu_1+\nu_2)R^*\right]$. Thus, with sufficient data, many temperature- and molality-dependent binary activity coefficients can be written in terms of equations (26) and (27). Table 1 lists B, G, and H values for 10 electrolytes and the range of validity for data. Since polynomial fits tend to wander off in random directions when the molality increases much beyond the limit of the given data, activity values from the last valid molality are used when modeling.

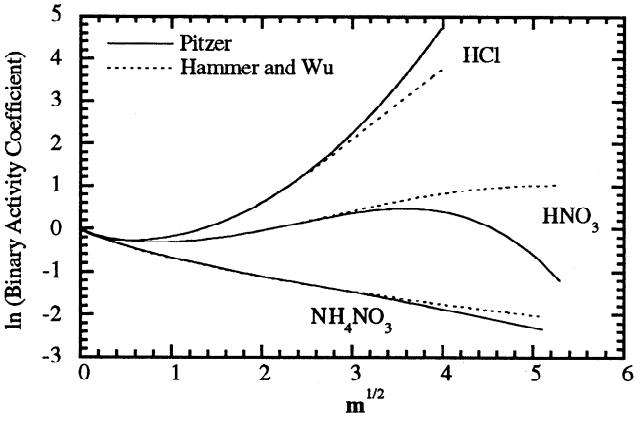

Figure 1. Comparison of mean binary activity coefficient data measured by *Hamer and Wu* [1972] to those computed using the Pitzer [1991] method.

Obtaining the temperature-dependent mean binary activity coefficients of bisulfate and sulfate is more difficult. When sulfuric acid dissolves in water, the resulting mixture contains both sulfate and bisulfate ions. The *Pitzer et al.* [1977] model, which is valid from 0 - 6 m and for temperatures down to 273 K, describes how to obtain the molalities and activity coefficients of the two ions together in such a mixture. *Clegg and Brimblecombe* [1995] determined bisulfate and sulfate mixed activity coefficients for 0 - 40 m and < 200 K - 328 K. However, for Bromley's mixed-electrolyte model, activity coefficients of bisulfate and sulfate, each isolated in solution, are needed. The Kusik and Meissner [1978] model, as applied by *Stelson et al.* [1984], mathematically isolates binary activity coefficients given mixed activity coefficients, such as those calculated by the models of Pitzer *et al.* and Clegg and Brimblecombe.

Thus, to find temperature-dependent binary activity coefficients of bisulfate and sulfate, equations from the model of *Clegg and Brimblecombe* [1994] were combined with equations (72) and (73) of *Stelson et al.* in a Newton-Raphson iteration. The results were tabulated for the temperature range < 201 - 328 K and the molality range 0 - 40 m so that values for specific molalities and temperatures can be interpolated when used in equilibrium equations. Figure 2 depicts how the isolated binary

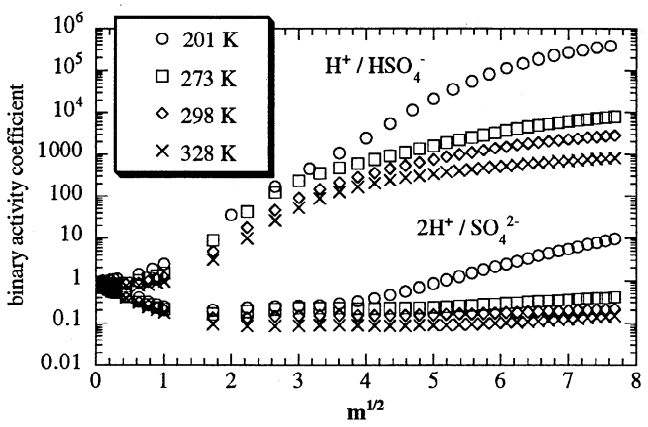

Figure 2. Mean binary activity coefficients of sulfate and bisulfate, each alone in solution.

activity coefficients of sulfate and bisulfate vary with molality and temperature.

The reason most activity coefficients are written in the form of simple polynomials or tabulated is to speed the solution of equilibrium equations over a large modeling domain. For example, during a model time interval, the temperature is usually known. Thus, equation (27) can be calculated once for each species at the beginning of each time interval. Subsequently, during the iteration of equilibrium equations, only equation (26) is solved to find mean binary activity coefficients.

4.3. Water Equation

When the model relative humidity (RH) exceeds 100%, the partial pressure of water exceeds the surface vapor pressure, and water condenses rapidly. In these cases an empirical surface vapor pressure for water is calculated and used in equations (8) and (9) to determine fog or cloud growth. When the RH is below 100%, solute lowers the surface vapor pressure of water over aerosols and permits condensation. In such cases, water vapor is assumed to be in equilibrium with the aerosol phase.

The empirical scheme used to calculate equilibrium liquid water content is the ZSR [*Zdanovskii,* 1948; *Robinson and Stokes,* 1964] method. With the ZSR method the mole concentration of water in a solution of mixed electrolytes is calculated as

$$c_w = \frac{1000}{M_w}\sum_{i=1}^{N_C}\left(\sum_{j=1}^{N_A}\frac{c_{(2i-1),(2j),x}}{m_{(2i-1),(2j),a}}\right), \qquad (28)$$

where c_w is the liquid water content (mol cm^{-3} air), N_C is the number of possible cation types in solution, N_A is the number of possible anion types, $c_{(2i-1),(2j),x}$ is the mole concentration (mol cm^{-3} air) of electrolyte $(2i-1),(2j)$ in a solution containing all electrolytes at the ambient water activity, and $m_{(2i-1),(2j),a}$ is the molality of the electrolyte if it were alone in solution at the ambient water activity (relative humidity).

Pilinis and Seinfeld gave polynomial expressions of water activity (equal to relative humidity) as a function of molality ($m_{i,0}$) for several electrolytes at 298 K. Much of these data was derived from *Cohen et al.* [1987a, b], *Bassett and Seinfeld* [1983], and *Pitzer and Mayorga* [1973]. Here, the polynomials were recomputed in the form

$$m_a^{1/2} = Y_0 + Y_1 a_w + Y_2 a_w^2 + Y_3 a_w^3 + \cdots, \qquad (29)$$

where a_w is the water activity (relative humidity expressed as a fraction), the Y values are parameters listed in Table 2, and m is the molality of the binary electrolyte alone in solution at the given relative humidity. Because equation (29) is calculated once for each humidity, only equation (28) needs to be iterated to find aerosol liquid water content during a given equilibrium solution sequence.

Unlike temperature dependence of binary solute activity coefficients, the temperature dependence of binary water activity coefficients under ambient surface conditions appears fairly small. For example, the temperature dependence of water activity [*Harned and Owen,* 1958] can be written as

$$\ln a_w(T) = \ln a_w^0 - \frac{M_w m^2}{1000R^*}\left[\frac{T_L}{T_0}\frac{\partial \phi_L}{\partial m} + T_C\frac{\partial \phi_{c_P}}{\partial m}\right]. \qquad (30)$$

If the water activity at the reference temperature is expressed as

$$\ln a_w^0 = A_0 + A_1 m^{1/2} + A_2 m + A_3 m^{3/2} + \cdots + \cdots, \qquad (31)$$

then equations (24), (25), (30), and (31) can be combined to form

$$\ln a_w(T) = A_0 + A_1 m^{1/2} + A_2 m + E_3 m^{3/2} + E_4 m^2 \cdots \qquad (32)$$

where

$$E_l = A_l - \frac{0.5(l-2)M_w}{1000R^*}\left[\frac{T_L}{T_0}U_{l-2} + T_C V_{l-2}\right] \qquad (33)$$

for each j greater than 2. Equation (32) shows that temperature affects the water-activity polynomial beginning only in the fourth term. In equation (26), temperature affected the solute activity beginning with the second term of the polynomial. At high molalities (above 10 m) and at ambient surface temperatures (273 - 310 K), temperature only slightly affects water activity. For example, at 16 m, HCl gives a binary water activity of 0.09 when T = 273 K and an activity of about 0.11 when 310 K. At lower molalities, temperature has even less of an effect.

4.4. Deliquescence Relative Humidities

The code treats the formation of secondary, inorganic solids. A secondary solid cannot precipitate in a particle when the ambient relative humidity is greater than the deliquescence relative humidity (DRH) of the solid. Further, when the relative humidity is below the DRH, the solid may or may not form, depending on other equilibrium constraints. Finally, the DRH of the solid in equilibrium with a multicomponent mixture is lower than the DRH of the solid alone [*Wexler and Seinfeld,* 1991; *Tang and Munkelwitz,* 1993]. However, in the absence of detailed deliquescence information it is assumed that a solid might form if the relative humidity drops below the DRH of the solid in a multicomponent solution.

In the code, temperature-dependent DRH data for NaCl, $NaNO_3$, NH_4Cl, NH_4NO_3, and $(NH_4)_2SO_4$ are used from *Wexler and Seinfeld* [1991]. In addition, DRHs at 298 K for $NaHSO_4$, $NaNO_3$, and $(NH_4)_2SO_4$ were obtained from *Pilinis and Seinfeld* [1987]. Solids in the model are assumed to precipitate from ion-ion or aqueous-aqueous equilibrium reactions. At the beginning of an equilibrium calculation, all existing solid electrolytes are assumed to be dissociated. If the relative humidity is sufficiently low, the equilibrium relations will predict one or more solids to form and liquid water content to decrease, even to zero if appropriate.

Table 2. Parameters for Calculating Molalities of Binary Electrolytes as a Function of Relative Humidity

Species Low RH / High m	HCl 0% RH, 18.5 m	HNO_3 0% RH, 22.6 m	H^+/HSO_4^- 0% RH, 29.1 m	$2H^+ / SO_4^{2-}$ 0% RH, 29.1 m
Y_0	4.382962 (0)	4.852977 (0)	5.611895 (0)	5.611895 (0)
Y_1	-5.357632 (0)	-6.621314 (0)	-1.387446 (1)	-1.387446 (1)
Y_2	3.098542 (1)	3.390133 (1)	1.750682 (1)	1.750682 (1)
Y_3	-2.000641 (2)	-1.985191 (2)	7.138146 (1)	7.138146 (1)
Y_4	6.504476 (2)	6.281150 (2)	-3.109173 (2)	-3.109173 (2)
Y_5	-1.081413 (3)	-1.038494 (3)	4.662288 (2)	4.662288 (2)
Y_6	8.842283 (2)	8.498917 (2)	-3.128612 (2)	-3.128612 (2)
Y_7	-2.829861 (2)	-2.729090 (2)	7.767097 (1)	7.767097 (1)
Species Low RH / High m	NaCl 43% RH, 13.6 m	$NaNO_3$ 46% RH, 40 m	$NaHSO_4$ 0% RH, 20.5 m	Na_2SO_4 51% RH, 12.8 m
Y_0	-1.918004 (2)	4.976285 (3)	4.662777 (0)	-3.295311 (3)
Y_1	2.001540 (3)	-4.971878 (4)	-1.128472 (1)	3.188349 (4)
Y_2	-8.557205 (3)	2.099707 (5)	7.049464 (1)	-1.305168 (5)
Y_3	1.987670 (4)	-4.855791 (5)	-2.788050 (2)	2.935608 (5)
Y_4	-2.717192 (4)	6.648387 (5)	6.103105 (2)	-3.920423 (5)
Y_5	2.187103 (4)	-5.396606 (5)	-7.409417 (2)	3.109519 (5)
Y_6	-9.591577 (3)	2.407868 (5)	4.614577 (2)	-1.356439 (5)
Y_7	1.763672 (3)	-4.561394 (4)	-1.150735 (2)	2.510249 (4)
Species Low RH / High m	NH_4Cl 47% RH, 23.2 m	NH_4NO_3 62% RH, 28 m	NH_4HSO_4 0% RH, 31.2 m	$(NH_4)_2SO_4$ 47% RH, 17.9 m
Y_0	5.499544 (2)	1.235157 (4)	5.515580 (0)	4.363511 (2)
Y_1	-6.162768 (3)	-1.097966 (5)	3.588744 (0)	-4.947645 (3)
Y_2	2.954960 (4)	4.173924 (5)	-6.363443 (1)	2.399693 (4)
Y_3	-7.757513 (4)	-8.792165 (5)	3.687630 (2)	-6.364664 (4)
Y_4	1.202065 (5)	1.108433 (6)	-1.023972 (3)	9.952891 (4)
Y_5	-1.099605 (5)	-8.364973 (5)	1.394436 (3)	-9.179112 (4)
Y_6	5.502138(4)	3.499527 (5)	-9.168213 (2)	4.626748 (4)
Y_7	-1.162895 (4)	-6.261910 (4)	2.328726 (2)	-9.844195 (3)

Read 1.23 (0) as 1.23 x 10^0. The Y coefficients fit into equation (29). The table also lists the lowest relative humidity (RH) and corresponding highest molality that each fit is valid for.

4.5. Computer Optimization

Iterating equilibrium equations in a model with many grid cells, especially while solving for activities and the water content of an aerosol, is a slow process. Thus, steps are taken here to reduce time. The first is to vectorize the computer code around the grid-cell dimension on vectorized computers. Dividing the "grid domain" (all grid cells) into "grid blocks" (groups of grid cells) and vectorizing around the cells in each block permits code speedups by a factor of 30 or more compared to not vectorizing [*e.g.*, *Jacobson and Turco*, 1994]. To vectorize in such a manner, the calculation sequence must be the same in each grid cell. This is accomplished by iterating all equations in a block until the stiffest cell converges. While the extra iterations in the already converged grid cells may be unnecessary, the speedup from vectorization almost always outweighs the loss in speed due to excess computations.

If gas-aerosol equilibrium equations are solved, then another measure can be taken to speed the solver, which is to solve equations of the form A(g)<=>B(aq), without iteration. The direct equilibrium solution is $c_{B,eq} = \left(C_{A,0} + c_{B,0}\right) K_{eq} / \left(1 + K_{eq}\right)$ and $C_{A,eq} = c_{B,eq} / K_{eq}$, where the superscript 0 denotes the initial concentration. More complex equilibrium equations can be solved without iteration; however, even with 14 digits of computer accuracy, roundoff error makes some solutions very inaccurate. Excessive roundoff errors usually occur within the quadratic equation that arise for many of these solutions. Since the error often occurs within the square-root term, common techniques to avoid roundoff error often do not help. Even the simple Henry's-law-type equation above is subject to some roundoff errors.

5. Equilibrium Code Results

5.1. Simulations

Figure 3 shows the ability of EQUISOLV to converge more than 1400 equilibrium equations simultaneously. The figure shows concentrations of three gases and total liquid water converging in a system containing 21 gases, 30 aerosol size bins,

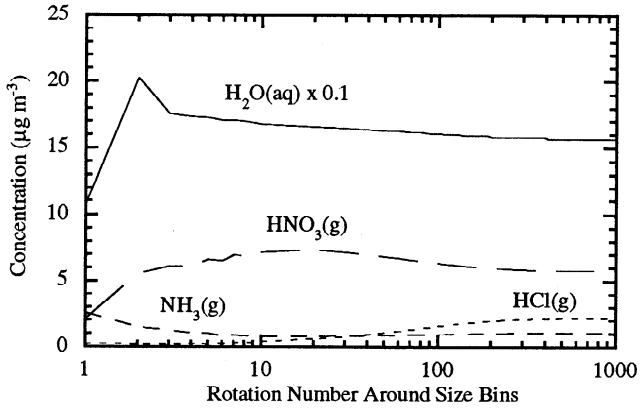

Figure 3. Convergence of three gases and liquid water during a test where equilibrium was solved among 21 gases and 46 aerosol species in each of 30 aerosol size bins. Conditions are described in the text. Convergence occurred after about 250 marches around all equations and size bins. Each equation, itself, was either iterated or solved in a one-step calculation.

Table 3. Aqueous, Ionic, and Solid Species Used in Equilibrium Equations of Table 4

Chemical Formula	Chemical Name	Chemical Formula	Chemical Name
$H_2O(aq)$	water	Na^+	sodium ion
$H_2SO_4(aq)$	sulfuric acid	Cl^-	chloride ion
$HNO_3(aq)$	nitric acid	$Na_2SO_4(s)$	sodium sulfate
$NH_3(aq)$	ammonia	$NaHSO_4(s)$	sodium bisulfate
$HCl(aq)$	hydrochloric acid	$NaCl(s)$	sodium chloride
H^+	hydrogen ion	$NaNO_3(s)$	sodium nitrate
OH^-	hydroxy ion	$(NH_4)_2SO_4(s)$	ammonium sulfate
NH_4^+	ammonium ion	$NH_4HSO_4(s)$	ammonium bisulfate
NO_3^-	nitrate ion	$NH_4Cl(s)$	ammonium chloride
HSO_4^-	bisulfate	$NH_4NO_3(s)$	ammonium nitrate
SO_4^{2-}	sulfate		

46 aerosol species in each size bin, where 47 equilibrium equations were solved within each bin (total of 1401 components and 1410 equilibrium equations converged). Table 3 gives a short list of some of the aqueous phase species in each size bin. Table 4 shows some of the equilibrium equations solved for. All 21 gases were initialized with mass concentrations (*e.g.*, 10 $\mu g\ m^{-3}\ NH_3$, 30 $\mu g\ m^{-3}\ HNO_3$). However, the only species initialized in the aerosol phase were sulfate (10 $\mu g\ m^{-3}$) and sodium chloride (10 $\mu g\ m^{-3}$), both of which were given trimodal distributions. Most sulfate was placed in the accumulation mode and most sodium chloride was placed in the coarse particle mode. For this simulation the normalized gross error of all gas concentrations reached 10^{-4} after about 500 marches around the size bins.

Second, a result from EQUISOLV was compared to a figure from *Pilinis and Seinfeld* (P&S) [1987]. Figure 4 shows a case where the initial conditions, equilibrium equations, equilibrium constants, and activity data were the same as in Figure 1 of P&S. In this case, the relative humidity was 90% and gases were equilibrated with one aerosol size bin. The results from EQUISOLV matched those from P&S.

Third, Figure 5 shows a model simulation of the change in aerosol composition as a function of relative humidity. As humidity decreased from 100%, water, chlorine, nitrate, and ammonium decreased steadily. At about 62% humidity, which is near the deliquescence humidity of ammonium nitrate, both ammonium nitrate and ammonium sulfate precipitated. Ammonium sulfate did not precipitate at higher relative humidities although its DRH was about 80% because it was undersaturated at higher humidities. Above its DRH a solid may not precipitate; below its DRH a solid may or may not precipitate, depending upon other equilibrium constraints [*Pilinis and Seinfeld*, 1987]. Ammonium sulfate can remain in the aqueous phase until the relative humidity decreases below 30% [*Tang*, 1980].

Finally, Table 5 shows gas and particle composition predictions at equilibrium for different liquid water contents. The first case is for aerosols at 90% humidity, the second case is for fog drops that formed when the relative humidity was increased instantaneously to 100.4%, and the third case is for cloud drops that formed when the relative humidity was increased instantaneously to 101.9%. For the sub-100% humidity case, liquid water content and composition were determined solely by equilibrium calculations. These results are similar to the NaCl = 15 $\mu g\ m^{-3}$ case in Figure 4, except that here, HSO_4^- was included

Table 4. List of some equilibrium reactions and constants

	Reaction	A	B	C	Units	ref.
1	$HNO_3(g) \Leftrightarrow HNO_3(aq)$	2.10 (5)			mole kg^{-1} atm^{-1}	E
2.	$NH_3(g) \Leftrightarrow NH_3(aq)$	5.76 (1)	13.79	-5.39	mole kg^{-1} atm^{-1}	H
3.	$HNO_3(g) \Leftrightarrow NO_3^- + H^+$	2.51 (6)	29.17	16.83	$mole^2\ kg^{-2}\ atm^{-1}$	H
4.	$NH_3(g) + HNO_3(g) \Leftrightarrow NH_4^+ + NO_3^-$	2.59 (17)	63.98	11.44	$mole^2\ kg^{-2}\ atm^{-2}$	*
5.	$NH_3(g) + HCl(g) \Leftrightarrow NH_4^+ + Cl^-$	2.03 (17)	65.01	14.52	$mole^2\ kg^{-2}\ atm^{-2}$	*
6.	$HCl(g) \Leftrightarrow Cl^- + H^+$	1.97 (6)	30.2	19.91	$mole^2\ kg^{-2}\ atm^{-1}$	H
7.	$H_2O(aq) \Leftrightarrow H^+ + OH^-$	1.01 (-14)	-22.52	26.92	mole kg^{-1}	H
8	$HNO_3(aq) \Leftrightarrow NO_3^- + H^+$	1.20 (1)	29.17	16.83	mole kg^{-1}	*
9	$NH_3(aq) + H_2O(aq) \Leftrightarrow NH_4^+ + OH^-$	1.81 (-5)	-1.50	26.92	--	H
10.	$NH_3(aq) + HNO_3(aq) \Leftrightarrow NH_4^+ + NO_3^-$	2.14 (10)	50.19	16.83	--	*
11.	$HCl(aq) \Leftrightarrow Cl^- + H^+$	1.72 (6)	23.15		mole kg^{-1}	S
12.	$H_2SO_4(aq) \Leftrightarrow HSO_4^- + H^+$	1.00 (3)			mole kg^{-1}	T
13	$HSO_4^- + H^+ \Leftrightarrow SO_4^{2-} + 2\ H^+$	1.02 (-2)	8.85	25.14	mole kg^{-1}	H
14.	$NH_4HSO_4(s) \Leftrightarrow NH_4^+ + HSO_4^-$	1.38 (4)	-2.87	15.83	$mole^2\ kg^{-2}$	H
15.	$(NH_4)_2SO_4(s) \Leftrightarrow 2\ NH_4^+ + SO_4^{2-}$	1.82 (0)	-2.65	38.57	$mole^3\ kg^{-3}$	H
16.	$NH_4Cl(s) \Leftrightarrow NH_4^+ + Cl^-$	2.21 (1)	-6.03	16.92	$mole^2\ kg^{-2}$	*
17.	$NH_4NO_3(s) \Leftrightarrow NH_4^+ + NO_3^-$	1.49 (1)	-10.4	17.56	$mole^2\ kg^{-2}$	*
18	$NaHSO_4(s) \Leftrightarrow Na^+ + HSO_4^-$	2.41 (4)	0.79	14.75	$mole^2\ kg^{-2}$	H
19.	$Na_2SO_4(s) \Leftrightarrow 2\ Na^+ + SO_4^{2-}$	4.80 (-1)	0.98	39.57	$mole^3\ kg^{-3}$	H
20	$NaCl(s) \Leftrightarrow Na^+ + Cl^-$	3.77 (1)	-1.56	16.9	$mole^2\ kg^{-2}$	H
21	$NaNO_3(s) \Leftrightarrow Na^+ + NO_3^-$	1.20 (1)	-8.22	16.01	$mole^2\ kg^{-2}$	H

Read 1.23 (0) as 1.23×10^0. E, *Schwartz* [1984]; H, *Kim et al.* [1993]; S, *Marsh and McElroy* [1985]; T, *Perrin* [1982]; Asterisk, rates were combined from a combination of other rates in the table or not included in the table. The equilibrium constant reads $K_{eq}(T) = Ae^{\left[B(T_o/T-1)+C\left(1+\ln(T_o/T)-T_o/T\right)\right]}$, where $A = K_{eq}(T_o)$, T_o is the reference temperature (298.16 K), T is temperature (K), $B = -\Delta H^\circ_{T_o} / R^* T_o$, and $C = -\Delta c_p^\circ / R^*$.

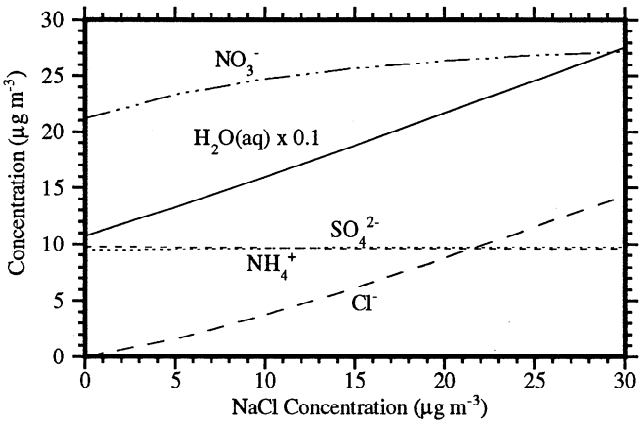

Figure 4. Aerosol composition versus NaCl concentration when the relative humidity was 90%. Other initial conditions were $H_2SO_4(aq) = 10\ \mu g\ m^{-3}$, $HCl(g) = 0\ \mu g\ m^{-3}$, $NH_3(g) = 10\ \mu g\ m^{-3}$, $HNO_3(g) = 30\ \mu g\ m^{-3}$, and T = 298 K. Compare to *Pilinis and Seinfeld* [1987], Figure 1.

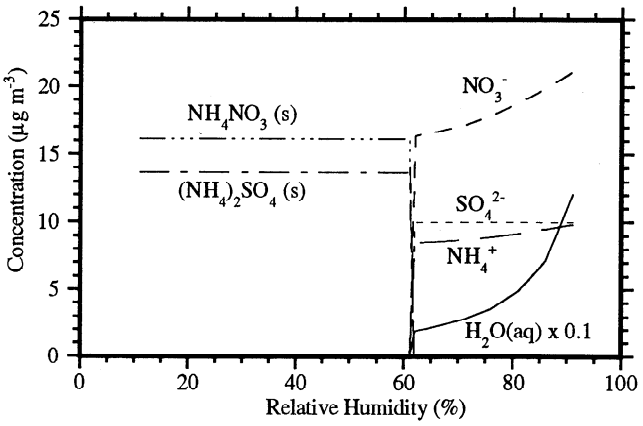

Figure 5. Aerosol composition versus relative humidity. Initial conditions were $H_2SO_4(aq) = 10\ \mu g\ m^{-3}$, $HCl(g) = 0\ \mu g\ m^{-3}$, $NH_3(g) = 10\ \mu g\ m^{-3}$, $HNO_3(g) = 30\ \mu g\ m^{-3}$, and $T = 298$ K.

as a component. Liquid water contents in the fog and cloud cases were determined by solving equations (8) and (9) for liquid water over 43 size bins until the relative humidity dropped to 100%. Composition at equilibrium was then determined by EQUISOLV.

An interesting feature of the result is that bisulfate concentrations ($\mu g\ m^{-3}$) increased, then decreased, and sulfate concentrations decreased, then increased as liquid water content increased. The reason appears to be that at low aerosol liquid water contents (high molalities), mean binary activity coefficients of bisulfate are high relative to those of sulfate (Figure 2), favoring sulfate at the expense of bisulfate molalities and concentrations. As liquid water contents increased from aerosol to fog-sized drops, bisulfate molalities and binary activity coefficients decreased, favoring bisulfate relative to sulfate. As water contents increased further, from fog- to cloud-sized drops, bisulfate molalities and mean binary activity coefficients changed only moderately; however, the *p*H of solution increased, favoring sulfate over bisulfate formation. Between aerosol and fog sizes, *p*H also increased; however, the effect of high bisulfate binary activity coefficients outweighed the effect of *p*H increases at these water contents.

5.2. Timing Tests

The time to solve equilibrium equations varies significantly, depending on the number of equations and size bins, the length of time intervals, and the value of error tolerances. To give an indication of program speed, a comparison to a timing test from another code is shown.

Table 7 of *Kim et al.* [1993b] gives timings of simulations for four cases. Here, their cases 3 and 4 are compared. The times for the equilibrium model, SCAPE, to solve the equations for their cases for one size bin, one time step, and a convergence criteria of 10^{-3} for gases and water, were 6.3 and 42 s, respectively, on a SUN SPARC station SLC. Since these tests, speeds of SCAPE have most likely been improved. For the same conditions and cases the times EQUISOLV took to obtain a normalized gross error in gas and liquid water concentrations of 10^{-4} on a nearly equivalent workstation (SUN SPARC station 1+) were 0.068 and 0.62 s, respectively. For EQUISOLV the same equations were

Table 5. Equilibrium Partitioning of Mass Between Particle and Gas Phases for Different Atmospheric Liquid Water Contents

	Aerosol		Fog		Cloud	
	$\mu g\ m^{-3}$	% of aerosol mass	$\mu g\ m^{-3}$	% of fog mass	$\mu g\ m^{-3}$	% of cloud mass
$H_2O(aq)$	1.83×10^2	76.694	9.43×10^4	99.931	4.37×10^5	99.985
H^+	0.00129	0.000541	0.0886	0.0000938	0.0928	0.0000212
NH_4^+	9.25	3.87	10.5	0.0112	10.5	0.00241
NO_3^-	24.5	10.3	29.5	0.0313	29.5	0.00675
HSO_4^-	0.247	0.103	0.557	0.000612	0.165	0.0000378
SO_4^{2-}	9.55	4.00	9.22	0.00977	9.63	0.00220
Na^+	5.90	2.47	5.90	0.00625	5.90	0.00135
Cl^-	6.19	2.59	9.10	0.00964	9.10	0.00208
*p*H	2.15		3.03		3.67	
$HNO_3(g)$	5.08		0.00408		0.000217	
$NH_3(g)$	1.26		0.0438		0.0421	
HCl(g)	2.99		0.00163		0.0000863	

The water content for the aerosol case was calculated at 90% relative humidity. Fog and cloud water contents were determined by solving equations (8) and (9) over a trimodal size distribution at relative humidities of 100.4 and 101.9%, respectively. Equilibrium compositions were solved for and summed over all size bins. Other initial conditions were $H_2SO_4(aq) = 10\ \mu g\ m^{-3}$, $HCl(g) = 0\ \mu g\ m^{-3}$, $NH_3(g) = 10\ \mu g\ m^{-3}$, $HNO_3(g) = 30\ \mu g\ m^{-3}$, NaCl = 15 $\mu g\ m^{-3}$, and $T = 298$ K. The aerosol case is similar to the NaCl(aq) = 15 $\mu g\ m^{-3}$ case shown in Figure 4.

solved in 1000 grid cells and the total time was divided by 1000 to obtain the time to solve in one grid cell.

6. Conclusion

A new chemical equilibrium solver and a modified method of coupling equilibrium calculations to growth calculations was discussed. The solver converges any number of gas, aqueous, ionic, or solid equilibrium equations while determining aerosol liquid water content and mean mixed activity coefficients. An application of the code is to estimate particle surface vapor pressures for use in growth equations. Vapor pressures can be predicted when particles contain only a solution phase, both a solution and solid phase, or only a solid phase. A second application of the equilibrium solver is to estimate particle composition and size after gas-aerosol transfer has occurred.

Finally, polynomial expressions for temperature-dependent binary activity coefficients were introduced. While a significant amount of data for relative apparent molal enthalpy, apparent molal heat capacity, and binary activity coefficients at 298 K are available for some species, more data are needed for other species and for solutions at high ionic strength.

Acknowledgments. A portion of this work was performed on a Cray J-916, provided in part by Cray Research, Inc. Cray 90 computer support was also given by the San Diego Supercomputer Center, the EPA Supercomputer Center at Bay City, Michigan, and the NAS computer facilities in Mountain View, California. This work was also supported, in part, by grants from the Environmental Protection Agency under assistance agreements 823755-01-0 (Atmos. Res. and Exposure Assessment Lab.) and 823186-01-0 (Nat'l Center for Environ. Research and Quality Assurance), the Charles Lee Powell Foundation, and the National Science Foundation under agreement ATM-9504481. Although the research described in this article has been funded in part by the United States Environmental Protection Agency, it has not been subjected to the Agency's peer and administrative review and therefore may not necessarily reflect the views of the Agency and no official endorsement should be inferred. Finally, we thank S. Clegg for providing a sulfuric acid activity coefficient model.

References

Allen, A. G., R. M. Harrison, and J. Erisman, Field measurements of the dissociation of ammonium nitrate and ammonium chloride aerosols, *Atmos. Environ.*, *17*, 1591 - 1599, 1989.

Bassett, M. E., and J. H. Seinfeld, Atmospheric equilibrium model of sulfate and nitrate aerosol, *Atmos. Environ.*, *17*, 2237 - 2252, 1983.

Bassett, M. E., and J. H. Seinfeld, Atmospheric equilibrium model of sulfate and nitrate aerosol, II, Particle size analysis, *Atmos. Environ.*, *18*, 1163 - 1170, 1984.

Bolsaitis, P., and J. F. Elliott, Thermodynamic activities and equilibrium partial pressures for aqueous sulfuric acid solutions, *J. Chem. Eng. Data*, *35*, 69 - 85, 1990.

Bolton, D., The computation of equivalent potential temperature, *Mon. Weather Rev.*, *108*, 1046 - 1053, 1980.

Bott, A., and G. R. Carmichael, Multiphase chemistry in a microphysical radiation fog model -- A numerical study, *Atmos. Environ.*, *27A*, 503 - 522, 1993.

Bromley, L. A., Thermodynamic properties of strong electrolytes in aqueous solutions, *AIChE J.*, *19*, 313 - 320, 1973.

Chameides, W. L., The photochemistry of a remote marine stratiform cloud, *J. Geophys. Res.*, *89*, 4739 - 4755, 1984.

Clegg, S. L., and P. Brimblecombe, Equilibrium partial pressures and mean activity and osmotic coefficients of 0 - 100% nitric acid as a function of temperature, *J. Phys. Chem.*, *94*, 5369 - 5380, 1990.

Clegg, S. L., and P. Brimblecombe, Application of a multicomponent thermodynamic model to activities and thermal properties of 0 - 40 mol kg^{-1} aqueous sulphuric acid from < 200 K to 328 K, *J. Chem. Eng. Data*, 40, 43 - 64, 1995.

Cohen, M. D., R. C. Flagan, and J. H. Seinfeld, Studies of concentrated electrolyte solutions using the electrodynamic balance, 1, Water activities for single-electrolyte solutions, *J. Phys. Chem.*, *91*, 4563 - 4574, 1987a.

Cohen, M. D., R. C. Flagan, and J. H. Seinfeld, Studies of concentrated electrolyte solutions using the electrodynamic balance, 2, Water activities for mixed-electrolyte solutions, *J. Phys. Chem.*, *91*, 4575 - 4582, 1987b.

Drdla, K., A. Tabazadeh, R. P. Turco, M. Z. Jacobson, J. E. Dye, C. Twohy and D. Baumgardner, Analysis of the physical state of one Arctic polar stratospheric cloud based on observations, *Geophys. Res. Lett.*, *21*, 2475 - 2478, 1994.

Filippov, V. K., M. V. Charykova, and Y. M. Trofimov, Thermodynamics of the system $NH_4H_2PO_4$-$(NH_4)_2SO_4$-H_2O at 25°C, *J. Appl. Chem. U.S.S.R.*, *58*, 1807, 1985.

Goldberg, R. N., Evaluated activity and osmotic coefficients for aqueous solutions: Thirty-six uni-bivalent electrolytes, *J. Phys. Chem. Ref. Data.*, *10*, 671 - 764, 1981.

Hamer, W. J., and Y.-C. Wu, Osmotic coefficients and mean activity coefficients of uni-univalent electrolytes in water at 25°C, *J. Phys. Chem. Ref. Data*, *1*, 1047 - 1099, 1972.

Harned, H. S., and B. B. Owen, *The Physical Chemistry of Electrolyte Solutions*, chap. 8, Van Nostrand, New York, 1958.

Harrison, R. M., and A. R. MacKenzie, A numerical simulation of kinetic constraints upon achievement of the ammonium nitrate dissociation equilibrium in the troposphere, *Atmos. Environ.*, *24A*, 91 - 102, 1990.

Harvie, C. E., N. Moller, and J. H. Weare, The prediction of mineral solubilities in natural waters: The Na-K-Mg-Ca-H-Cl-SO_4-OH-HCO_3-CO_3-CO_2-H_2O system to high ionic strengths at 25°C, *Geochim. et Cosmochim. Acta*, *48*, 723 - 751, 1984.

Hildemann, L. M., A. G. Russell, and G. R. Cass, Ammonia and nitric acid concentrations in equilibrium with atmospheric aerosols: Experiment vs. theory, *Atmos. Environ.*, *18*, 1737 - 1750, 1984.

Holmes, H. F., and R. E. Mesmer, Thermodynamics of aqueous solutions of the alkali metal sulfates, *J. Solution Chem.*, *15*, 495 - 518, 1986.

Jacob, D., Chemistry of OH in remote clouds and its role in the production of formic acid and peroxymonosulfate, *J. Geophys. Res.*, *91*, 9807 - 9826, 1986.

Jacobson, M. Z., and R. P. Turco, SMVGEAR: A sparse-matrix, vectorized Gear code for atmospheric models, *Atmos. Environ.*, *28A*, 273 - 284, 1994.

Jacobson, M. Z., and R. P. Turco, Simulating condensational growth, evaporation, and coagulation of aerosols using a combined moving and stationary size grid, *Aerosol Sci. Technol*, *22*, 73 - 92, 1995.

Jacobson, M. Z., Developing, coupling, and applying a gas, aerosol, transport, and radiation modeling system for studying urban and regional air pollution, Ph.D. thesis, Univ. of Calif., Los Angeles, 1994.

Jacobson, M. Z., Computation of global photochemistry with SMVGEAR II, *Atmos. Environ.*, *29A*, 2541 - 2546, 1995.

Kim, Y. P., J. H. Seinfeld, and P. Saxena, Atmospheric gas-aerosol equilibrium, I, Thermodynamic model, *Aerosol Sci. Technol.*, *19*, 157 - 181, 1993a.

Kim, Y. P., J. H. Seinfeld, and P. Saxena, Atmospheric gas-aerosol equilibrium, II, Analysis of common approximations and activity coefficient calculation methods, *Aerosol Sci. Technol.*, *19*, 182 - 198, 1993b.

Kusik, C. L., and H. P. Meissner, Electrolyte activity coefficients in inorganic processing, *AIChE Symp. Ser.*, *173*, 14 - 20, 1978.

Lide, D.R. (ed.), *CRC Handbook of Chemistry and Physics*, CRC Press, Boca Raton Fla., 1993.

Marsh, A. R. W., and W. J. McElroy, The dissociation constant and Henry's law constant of HCl in aqueous solution, *Atmos. Environ.*, *19*, 1075 - 1080, 1985.

Pandis, S. N., and J. H. Seinfeld, Sensitivity analysis of a chemical mechanism for aqueous phase atmospheric chemistry, *J. Geophys. Res.*, *94*, 1105 - 1126, 1989.

Parker, V. B., *Thermal Properties of Aqueous Uni-univalent Electrolytes*, in *N. Stand. Ref. Data Ser.*, NBS 2, U. S. Govt. Print. Off., Washington, D. C., 1965.

Perrin D. D., *Ionization Constants of Inorganic Acids and Bases in Aqueous Solution*, 2nd ed., Pergamon, New York, 1982.

Perron, G., A. Roux, A., and J. E. Desnoyers, Heat capacities and volumes of NaCl, $MgCl_2$, $CaCl_2$, and $NiCl_2$ up to 6 molal in water, *Can J. Chem.*, *59*, 3049 - 3054, 1981

Pilinis, C., and J. H. Seinfeld, Continued development of a general equilibrium model for inorganic multicomponent atmospheric aerosols, *Atmos. Environ.*, *21*, 2453 - 2466, 1987.

Pilinis, C., and J. H. Seinfeld, Development and evaluation of an eulerian photochemical gas-aerosol model, *Atmos. Environ.*, *22*, 1985 - 2001, 1988.

Pilinis, C., J. H. Seinfeld, and C. Seigneur, Mathematical modeling of the dynamics of multicomponent atmospheric aerosols, *Atmos. Environ.*, *21*, 943 - 955, 1987.

Pilinis, C., J. H. Seinfeld, and D. J. Grosjean, Water content of atmospheric aerosols, *Atmos. Environ.*, *23*, 1601 - 1606, 1989.

Pitzer, K. S., Ion interaction approach: Theory and data correlation. In *Activity Coefficients in Electrolyte Solutions, 2nd ed.*, edited by K. S. Pitzer, CRC Press, Boca Raton, Fla., 1991.

Pitzer, K. S., and G. Mayorga, Thermodynamics of electrolytes, II, Activity and osmotic coefficients for strong electrolytes with one or both ions univalent, *J. Phys. Chem.*, *77*, 2300 - 2308, 1973.

Pitzer, K. S., R. R. Roy, and L. F. Silvester, Thermodynamics of electrolytes, 7, Sulfuric Acid, *J. Am. Chem. Soc.*, *99*, 4930 - 4936, 1977.

Robinson, R. A., and R. H. Stokes, *Electrolyte Solutions*, 2nd ed., Butterworths, London, 1964.

Roux, A., G. M. Musbally, G. Perron, J. E. Desnoyers, P. P. Singh, E. M. Woolley, and L. G. Hepler, Apparent molal heat capacities and volumes of aqueous electrolytes at 25°C: $NaClO_3$, $NaClO_4$, $NaNO_3$, $NaBrO_3$, $NaIO_3$, $KClO_3$, $KBrO_3$, KIO_3, NH_4NO_3, NH_4Cl, and NH_4ClO_4, *Can. J. Chem.*, *56*, 24 - 28, 1978.

Russell, A. G., and G. R. Cass, Verification of a mathematical model for aerosol nitrate and nitric acid formation and its use for control measure evaluation, *Atmos. Environ.*, *20*, 2011 - 2025, 1986.

Russell, A. G., G. J. McRae, and G. R. Cass, Mathematical modeling of the formation and transport of ammonium nitrate aerosol, *Atmos. Environ.*, *17*, 949 - 964, 1983.

Russell, A., K. McCue, and G. R. Cass, Mathematical modeling of the formation of nitrogen-containing air pollutants, 1, Evaluation of an Eulerian photochemical model, *Environ. Sci. Technol.*, *22*, 263 - 271, 1988.

Saxena, P., and T. W. Peterson, Thermodynamics of multicomponent electrolytic aerosols, *J. Colloid Interface Sci.*, *79*, 496 - 510, 1981.

Saxena, P., C. Seigneur, and T. W. Peterson, Modeling of multiphase atmospheric aerosols, *Atmos. Environ.*, *17*, 1315 - 1329, 1983.

Saxena, P., A. B. Hudischewskyj, C. Seigneur, and J. H. Seinfeld, A comparative study of equilibrium approaches to the chemical characterization of secondary aerosols, *Atmos. Environ.*, *20*, 1471 - 1483, 1986.

Saxena, P., P. K. Mueller, Y. P. Kim, J. H. Seinfeld, and P. Koutrakis, Coupling thermodynamic theory with measurements to characterize acidity of atmospheric particles, *Aerosol Sci. Technol.*, *19*, 279 - 293, 1993.

Schwartz, S. E., Gas- and aqueous-phase chemistry of HO_2 in liquid water clouds, *J. Geophys. Res.*, *89*, 11,589 - 11,598, 1984.

Schwartz, S. E., and J. E. Freiberg, Mass-transport limitation to the rate of reaction of gases in liquid droplets: Application to oxidation of SO_2 in aqueous solutions, *Atmos. Environ.*, *15*, 1129 - 1144, 1981.

Scott, W. D., and F. C. R. Cattell, Vapor pressure of ammonium sulfates, *Atmos. Environ.*, *13*, 307 - 317, 1979.

Seigneur, C., A model of sulfate aerosol dynamics in atmospheric plumes, *Atmospheric Environment*, *16*, 270 - 294, 1982.

Seigneur, C., and P. Saxena, A study of atmospheric acid formation in different environments, *Atmos. Environ.*, *18*, 2109 - 2124, 1984.

Stelson, A. W., and J. H. Seinfeld, Relative humidity and temperature dependence of the ammonium nitrate dissociation constant, *Atmos. Environ.*, *16*, 983 - 992, 1982a.

Stelson, A. W., and J. H. Seinfeld, Relative humidity and *p*H dependence of the vapor pressure of ammonium nitrate-nitric acid solutions at 25° C, *Atmos. Environ.*, *16*, 993 - 1000, 1982b.

Stelson, A. W., and J. H. Seinfeld, Thermodynamic prediction of the water activity, NH4NO3 dissociation constant, density and refractive index for the NH_4NO_3-$(NH_4)_2SO_4$-H_2O system at 25°C, *Atmos. Environ.*, *16*, 2507 - 2514, 1982c.

Stelson, A. W., S. K. Friedlander, and J. H. Seinfeld, A note on the equilibrium relationship between ammonia and nitric acid and particulate ammonium nitrate, *Atmos. Environ.*, *13*, 369 - 371, 1979.

Stelson, A. W., Bassett, M. E., and J. H. Seinfeld, Thermodynamic equilibrium properties of aqueous solutions of nitrate, sulfate and ammonium, in *Chemistry of Particles, Fogs and Rain*, edited by J. L. Durham, Butterworth-Heinemann, Newton, Mass., 1984.

Sukhatme, S. P., and N. Saikhedkar, Heat capacities of glycerol-water mixtures and aqueous solutions of ammonium sulfate, ammonium nitrate, and strontium nitrate, *Ind. J. Technol.*, *7*, 1 - 4, 1969.

Tabazadeh, A., R. P. Turco, and M. Z. Jacobson, A model for studying the composition and chemical effects of stratospheric aerosols, *J. Geophys. Res.*, *99*, 12,897 - 12,914, 1994a.

Tabazadeh, A., R. P. Turco, K. Drdla, and M. Z. Jacobson, A study of type I polar stratospheric cloud formation, *Geophys. Res. Lett.*, *21*, 1619 - 1622, 1994b.

Tang, I. N., Deliquescence properties and particle size change of hygroscopic aerosols in generation of aerosols, in *Generation of Aerosols and Facilities for Exposure Experiments*, edited by K. Willeke, pp. 153 - 167, Butterworth-Heinemann, Newton, Mass., 1980.

Tang, I. N., and H. R. Munkelwitz, Composition and temperature dependence of the deliquescence properties of hygroscopic aerosols, *Atmos. Environ.*, *27A*, 467 - 473, 1993.

Vanderzee, C. E., D. H. Waugh, and N. C. Haas, Enthalpies of dilution and relative apparent molar enthalpies of aqueous ammonium nitrate. The case of a weakly hydrolysed (dissociated) salt, *J Chem. Thermodyn..*, *12*, 21 - 25, 1980.Villars, D. S., A method of successive approximations for computing combustion equilibria on a high speed digital computer, *J. Phys. Chem.*, *63*, 521 - 525, 1958.

Wagman, D. D., W. H. Evans, V. B. Parker, R. H. Schumm, I. Halow, S. M. Bailey, K. L. Churney, and R. L. Nuttall, The NBS tables of chemical thermodynamic properties: Selected values for inorganic and C_1 and C_2 organic substances in SI units, *J. Phys. Chem. Ref. Data*, *11*, *Suppl. 2*, 1982.

Wexler, A. S., and J. H. Seinfeld, The distribution of ammonium salts among a size and composition dispersed aerosol, *Atmospheric Environment*, *24A*, 1231 - 1246, 1990.

Wexler, A. S., and J. H. Seinfeld, Second-generation inorganic aerosol model, *Atmos. Environ.*, *25A*, 2731 - 2748, 1991.

Wexler, A. S., and J. H. Seinfeld, Analysis of aerosol ammonium nitrate: Departures from equilibrium during SCAQS, *Atmos. Environ.*, *26A*, 579 - 591, 1992.

Wu, Y.-C., and W. J. Hamer, Revised values of the osmotic coefficients and mean activity coefficients of sodium nitrate in water at 25°C, *J. Phys. Chem. Ref. Data*, *9*, 513 - 518, 1980.

Zdanovskii, A. B., New methods of calculating solubilities of electrolytes in multicomponent systems, *Z. Fiz. Khim*, *22*, 1475 - 1485, 1948.

M. Z. Jacobson (corresponding author), Department of Civil Engineering, Stanford University, Stanford, CA 94305-4020 (email:jacobson@ce.stanford.edu)

A. Tabazadeh, NASA Ames Research Center, Mountain View, CA 94035-1000 (email:taba@sky.arc.nasa.gov)

R. P. Turco, Department of Atmospheric Sciences, University of California, Los Angels, 405 Hilgard Avenue, Los Angeles, CA 90024-1565 (email:turco@cisk.atmos.ucla.edu)

(Received November 17, 1994; revised January 10, 1996; accepted January 18, 1996.)